Alterations in Left Ventricular Contractility in Dystrobrevin-Knockout Mice Characterized by MR Tagging

W. Liu[1,2], J. Chen[1,2], S. A. Wickline[1,2], R. M. Grady[3], X. Yu[1,2]

[1]Cardiovascular MR laboratories, Cardiovascular Division, Washington University, St. Louis, MO, United States, [2]Department of Biomedical Engineering, Washington University, St. Louis, MO, United States, [3]Department of Pediatrics, Washington University, St. Louis, MO, United States

Introduction

The dystrophin-glycoprotein complex (DGC) maintains the structural integrity of the muscle fibers (skeletal and cardiac) by linking the intracellular cytoskeleton to the overlying basal lamina. The importance of this linkage is underscored by the fact that mutations in both dystrophin and transmembrane components of DGC lead to muscular dystrophy and cardiomyopathy in humans and rodents. Recent studies suggest that the DGC plays signaling roles as well as structural roles. Of critical importance is the well-characterized cytoplasmic protein, dystrophin. Dystrophin mediates structural functions, by binding to F-actin, and signaling functions, by binding to α-dystrobrevin and syntrophin, which anchor signaling molecules such as neuronal nitric oxide synthase (nNOS). The *mdx* mouse, a model of Duchenne muscular dystrophy, carries a nonsense mutation in the dystrophin gene that eliminates the expression of dystrophin. Our previous studies by MR tagging indicated that *mdx* mice exhibited decreased left ventricular (LV) torsion despite the lack of clinical apparent defects in ejection fraction [1]. However, it is not clear whether such changes were caused primarily by structural disruption or altered signaling functions. Recent analysis of α-dystrobrevin knockout mice (adbn$^{-/-}$) demonstrated that impaired signaling functions of the DGC also lead to muscular dystrophy and cardiomyopathy, despite maintained structural integrity [2].

In this study, we seek to elucidate whether adbn$^{-/-}$ mice manifest a different cardiac functional phenotype as compared with *mdx* mice. Such analysis will allow us to address differences in the pathogenesis of cardiomyopathy in *mdx* and adbn$^{-/-}$ mice.

Methods

MR imaging: Two months old adbn$^{-/-}$ mice (n=5) and age matched control mice (n=7) were scanned on a Varian 4.7T scanner with a 2.5 cm surface RF coil. Tagged images of five short-axis slices were acquired from apex to base with 1 mm slice thickness. The tagging sequence used a SPAMM1331 sequence applied twice immediately after the ECG trigger, yielding a two-dimensional tag grid in imaging plane. The tagging sequence was followed by gradient-echo cine sequence with the following imaging parameters: TR, R-R interval; TE, 3 ms; field of view, 4 cm × 4 cm; matrix size, 256×256; tagging resolution, 0.5 mm. Fifteen frames were acquired per cardiac cycle.The animals were kept warm by a blow drier during the acquisition.

Histology: Hearts were fixed in 10% formalin. The fixed hearts were sliced at 1mm thickness from base to apex along the LV long axis. The tissue sections were stained with Masson's trichrome for identification of myocardial lesions.

Data analysis: Images were analyzed with MATLAB-based software developed in our laboratory. Epicardial and endocardial borders were traced interactively using B-spline interpolation with 8 control points. Intersecting tag points were tracked semi-automatically with HARP-based approach. Subsequently, strains were calculated by 2D homogenous strain analysis. The two eigenvalues of the strain tensor were calculated to yield maximum stretching and maximum shortening. Myocardial twist was computed relative to the center of ventricular cavity. Positive twist indicated clockwise twist viewed from base.

Results

The heart rate of adbn$^{-/-}$ mice was slightly slower than that of the controls 317±23 BPM vs. 435±62 BPM ($p<0.01$), possibly due to the altered nitric oxide regulation of the heart rate. Adbn$^{-/-}$ mice did not present signs of hypertrophy or dilation. However, histological analysis revealed small areas of fibrotic lesions in adbn$^{-/-}$ mice. The heart weight/body weight ratio was similar between the two groups 0.52±0.6% vs. 0.51±0.4% (p=NS). Relative wall thickness, defined as the ratio of wall thickness to ventricular radius, was also similar 15±2% vs. 15±3% (p=NS). The ejection fraction of adbn$^{-/-}$ mice was statistically the same as that of the controls (61±3% vs. 59±5%, p=NS).

Compared to control mice, adbn$^{-/-}$ mice exhibited a significantly altered pattern of ventricular twist (Figure 1, left). LV twist was the same in adbn$^{-/-}$ and control mice at basal level. While both adbn$^{-/-}$ and control mice demonstrated continuous shift in LV twist from counterclockwise to clockwise twist from base to apex, the magnitude was significantly enhanced in adbn$^{-/-}$ mice. In control mice, the twist shifted from –4.6±1.3° at base to 7.9±1.6° at apex. In adbn$^{-/-}$ mice, twist change was from –4.1±0.9° at base to 12.6±1.8° at apex ($p<0.01$). To account for variations in ventricular size, LV torsion was calculated as the differences in the twist between basal and apical slices, normalized by the distance between the two slices. Figure 1 (middle) demonstrates that torsion was also increased in adbn$^{-/-}$ mice with a peak value of 4.3±0.6°/mm vs. 3.1±0.3°/mm in controls ($p<0.01$). Besides the changes in magnitude, the time course differed between the two groups: the peak time for LV torsion and apical twist was slightly delayed in adbn$^{-/-}$ mice.

adbn$^{-/-}$ mice also exhibited significantly enhanced regional deformation. The magnitude of maximum shortening (principal strain) was increased throughout the ventricle (Figure 1, right): -0.20±0.02 vs –0.18±0.02 for slice 1 (apex, p=0.05), -0.19±0.02 vs. –0.16±0.01 for slice 2 ($p<0.01$), -0.19±0.01 vs. –0.15±0.02 for slice 3 ($p<0.01$), -0.16±0.02 vs. –0.13±0.01 for slice 4 ($p<0.01$), -0.15±0.01 vs. –0.13±0.01 for slice 5 (base, $p<0.05$).

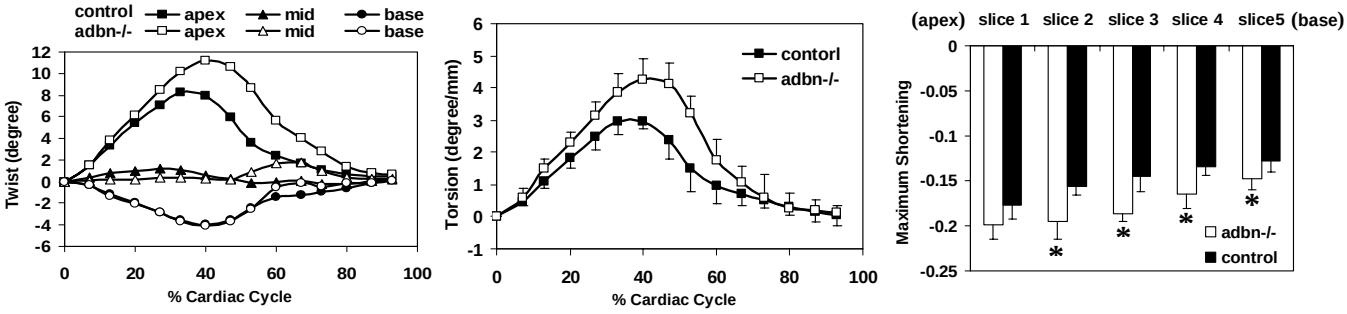

Figure 1. Left: Time course of LV twist. Middle: Time course of LV torsion. Right: Maximum LV shortening (* $p<0.05$).

Conclusion

Significant differences were observed in cardiac function in terms of twist and strain in adbn$^{-/-}$ mice despite the lack of differences in clinical indices of global cardiac function and anatomy. Interestingly, although adbn$^{-/-}$ mice developed similar patterns of cardiac lesions as *mdx* mice, the enhancement in torsion and strain in adbn$^{-/-}$ mice differed from that of *mdx* mice, which exhibited reduced torsion. The exact mechanisms underlying these differential changes remain to be elucidated. Our study indicates that functional adaptations to genetic mutations exhibit markedly different phenotypes in *mdx* and adbn$^{-/-}$ mice depending on the specific mutation.

References:

1. Yu. X., et al, Pro. Intl. Soc. Mag. Reson. Med. 10 (2002).
2. Grady R.M. et al, Nature Cell Biology, 1: 215-220, 1999